Role of hippocampal circKcnk9 in visceral hypersensitivity and anxiety comorbidity of Irritable Bowel Syndrome

yuan Liu (1409554480@qq.com)
Fujian Medical University https://orcid.org/0000-0002-9976-8057
Zhong Chen
Fujian Medical University
Wei Lin
First Affiliated Hospital of Fujian Medical University
Yifei Zhou
Fujian Medical University
Zihan Liu
Fujian Medical University
Ruixia Zhao
Fujian Medical University
Yu Chen
Fujian Medical University
Bin Wu
First Affiliated Hospital of Fujian Medical University
Aiqin Chen
Fujian Medical University
Chun Lin
Fujian Medical University https://orcid.org/0000-0002-7141-2446

Research Article

Keywords: CircKcnk9, MiR-124-3p, EZH2, Hippocampus, Irritable bowel syndrome

Posted Date: May 12th, 2022

DOI: https://doi.org/10.21203/rs.3.rs-1555945/v1

Abstract

Irritable bowel syndrome (IBS) is a prevalent functional disease. However, its molecular and pathological mechanisms are poorly understood. In this study, neonatal colorectal distension induced visceral hypersensitivity and anxiety comorbidity. The expression of hippocampal circKcnk9, a novel circRNA we termed, was increased significantly in IBS-like rats. Interesting, CA1 shcircKcnk9 treatment inhibited LTP and alleviated visceral hypersensitivity and anxiety in IBS-like rats while overexpression of CA1 circKcnk9 induced LTP, visceral hypersensitivity and anxiety in controls. Then, several experiments indicated that increased CA1 circKcnk9 acts as miR-124-3p sponge, which results in the inhibiting effect of miR-124-3p on gene silencing. There was a negative correlation between circKcnk9 and miR-124-3p. As expected, CA1 administration of agomiR-124-3p decreased CA1 LTP, visceral hypersensitivity and anxiety in IBS-like rats. In contrast, CA1 treatment with antagomiR-124-3p induced LTP, visceral hypersensitivity and anxiety in controls. Furthermore, bioinformatics analysis and experimental data showed EZH2 is a target gene of circKcnk9/miR-124-3p and increased EZH2 expression is involved in visceral hypersensitivity and anxiety of IBS-like rats by enhancing hippocampal synaptic plasticity.

In conclusion, early life stress induces increased expression of circKcnk9 in the CA1 of IBS-like rats. Increased circKcnk9 ensuing regulates the synaptic transmission and enhances LTP, leading to visceral hypersensitivity and anxiety comorbidity in IBS-like rats. The underlying signaling pathway of circKcnk9 is miR124-3p/EZH2. Increased circKcnk9 reinforces its sponge for miR124-3p, strongly suppresses miR124-3p activity, resulting in increased expression level of target gene EZH2. The study provides a new epigenetic mechanism of visceral hypersensitivity and anxiety comorbidity in IBS-like rats.

Introduction

Irritable bowel syndrome (IBS) is characterized by recurrent episodes of abdominal pain and irregular bowel habit without recognizable organic pathological changes. Patients with IBS often suffer negative emotional comorbidities such as anxiety and depression due to persistent visceral hypersensitivity[1–3]. Chronic exposure to adverse life events especially in the early stages increases personal susceptibility to IBS disorders[4]. However, the molecule mechanism involved in visceral hypersensitivity and emotional comorbidity of IBS remains unclear.

Long-lasting phenotypes such as chronic pain and emotional comorbidity may be associated with epigenetic modulation of gene expression[5]. Circular RNAs (circRNAs) seem to function as post-transcriptional regulatory molecules. CircRNAs are a type of noncoding RNA formed by a closed-loop structure without 5’ hat and 3’ polyadenylated tail. Ample evidence suggest that dysregulation of circRNAs is implicated in many diseases, inculding cancer[6, 7], chronic pain[8] and emotional comorbidity[9]. Different circRNAs are involved in different type of chronic pain. CircAnks1a regulats hypersensitivity in rodent models of neurological pain[10]. Cancer pain study found that circStrn3 is involved in the regulation of bone cancer pain in rats[11]. Recent data also support the regulation of circRNAs in negative emotions. CircSTAG1 was significantly decreased in the hippocampus of chronic

unpredictable stress-treated mouse and in peripheral blood of patients with major depressive disorder[9]. Visceral hypersensitivity and negative emotions are often comorbid with IBS. Our previous study demonstrated that long-term potentiation (LTP) is enhanced in the hippocampal CA1 of IBS-like rats[12], indicating early life stress results in abnormal synaptic plasticity and adverse memory in hippocampus. The hippocampus is associated with memory formation, visceral function and emotional modulation[13]. Several studies have suggested that hippocampal circRNA may be involved in the regulation of pain[14], negative emotions[9] and synaptic plasticity[15]. We hypothesized that early life stress induces abnormal expression of hippocampal circRNA, which regulates synaptic plasticity, consequently lead to visceral hypersensitivity and anxiety comorbidity in IBS-like rats. We found the expression of hippocampal circKcnk9, a novel circRNA we identified, was increased significantly in IBS-like rats. Literatures have been reported that circRNAs can act as miRNA sponges to modulate the expression of target genes[16, 17]. Mice exposed to chronic ultra-mild stress exhibited increased depression-like behaviors and reduced hippocampal expression of the brain-enriched miR-124[18]. In addition, miR-124-3p is involved in neuropathic pain in CCI rat models[19]. Furthermore, we used MiRanda database to predict the binding sites and found circKcnk9 has three binding sites for miR-124-3p. Literatures and bioinformatic result indicate miR-124-3p may act as miR-124-3p sponge in IBS-like rats, which needs more experiments to confirm.

In our study, we first determined the role of hippocampal circKcnk9 in the visceral hypersensitivity and anxiety of IBS-like rats. Then, we investigated whether circKcnk9 played its regulatory role as miR-124-3p sponge. Finally, we explored the downstream target gene of circKcnk9 and miR-124-3p using a variety of experimental methods. The study could provide a new epigenetic mechanism of visceral hypersensitivity and anxiety comorbidity in IBS-like rats.

Materials And Methods

Animals

Adult male Sprague-Dawley rats (body weight range: 180-220g) were obtained from the Department of Experimental Animal Center, Fujian Medical University. Animals were maintained in a specific pathogen-free-grade environment at the animal center. Weaning is typically initiated 21 days after birth. The experiments were approved by the Animal Care and Use Committee of Fujian Medical University. IBS-like rats were established by 60 mmHg colorectal distension (CRD) stimulation once daily during postnatal days 7–14[20]. We examined electromyographic (EMG) magnitude in response to graded strengths of CRD pressures in IBS-like rats and control rats at 6-8weeks to assess visceral sensitivity.

Stereotactic cannulation surgery and infusion

The rats were anesthetized with isoflurane (2%) and fixed on a stereotactic instrument (Ruiwode Life Science, China). Following routine skin sterilization, a scalp incision was made along the midline, and local anesthesia was performed with lidocaine. The skull was exposed and cleaned by scraping with 10%

hydrogen peroxide. All surgical procedures were performed under aseptic conditions, and no evidence of infection was detected.

The coordinates of the injection locations were centred at 4.0 mm in anteroposterior plane, 2.5 mm in mediolateral plane, and 2.8 mm in the dorsalventral plane. The rats underwent stereotaxic surgery for double cannula (inradium 2.8 mm, inner diameter: 0.3mm out diameter: 0.48mm, Ruiwode Life Science, China) implantation and were allowed to rest for at least 7 days. Continuous intrahippocampal administration (agomiR-124-3p/nc and SiEZH2 for IBS-like rats; antagomiR-124-3p/nc for controls) was administered once a day for 3 days.

The IBS-like rats that received intrahippocampal injection of LV-hSyn-mcherry-5'MiR-30a-shcirc7685 -3'MiR-30a-WPRE (shcircKcnk9, 1μL, Fig S1, BrainVTA, WuHan) were allowed to rest for postoperative 10 days. The control rats received intrahippocampal injection of aav-Kcnk9 virus (PFD-rAAV-hSyn-circ7685-nEF1a-EGFP-hGH, 1μL, Fig.S1, BrainVTA, WuHan) and were allowed to rest for postoperative 21 days (The timeline of this process is correlated with that of viral production).

The coordinates of the injection locations were centred at 4.0 mm in anteroposterior plane, 2.5 mm in mediolateral plane, and 2.8 mm in the dorsalventral plane. The rats underwent stereotaxic surgery for double cannula (inradium 2.8 mm, inner diameter: 0.3mm out diameter: 0.48mm, Ruiwode Life Science, China) implantation and were allowed to rest for at least 7 days. Continuous intrahippocampal administration (agomiR-124-3p/nc and SiEZH2 for IBS-like rats; antagomiR-124-3p/nc for controls) was administered once a day for 3 days.

Behavioral tests

All experiments were randomized. All behavioral tests were conducted between 13:00 and 16:00, and during the experiment, the experimental environment was maintained noise-free, and only 6–8-week-old male rats were used for behavioral assays. All animals were allowed to habituate for 1 h before behavioral testing. Videos were recorded and analyzed using video-tracking software (Yishu, Shanghai).

Open field test (OFT)

The novel environment was a black Plexiglas area (100cm × 100cm × 60cm). The equipment was wiped with 10% ethanol three times to eliminate odor clues between each rat. Rats were placed in the center of the Plexiglas area and allowed to freely explore the field for 5 min. Total travel distance, travel distance in the central area, and time spent in the central area were measured as indicators of anxiety.

Elevated plus maze test (EPM)

The EPM consisted of four arms: two open and two closed arms (LWH500 × 100 × 450mm). The rats were individually placed at the junction of the four arms at the beginning of the experiment. The equipment was wiped with 10% ethanol three times to eliminate odor clues between each rat. The tracking of rats was recorded for 5 min using video-tracking software and saved for future analysis on a computer. Additionally, the number of open-arm entries, open-arm time, and open-arm distance in EPM

were recorded for the indicators of anxiety-like behavior, as well as the number of times of arm openings, arm opening time, and arm opening distance in EPM as indicators of anxiety-like behavior. The video-tracking system was the same as that of the OFT analysis system.

Electromyography (EMG)

EMG was performed to assess visceral hypersensitivity. Rats (6–8 weeks old) were anesthetized with isoflurane. Prior to the CRD procedure, a glycerol-lubricated balloon was inserted into the rectum. A pair of bipolar electrodes were implanted in the abdominal external oblique musculature of shallow anesthetized rats to detect EMG activity. Under isoflurane superficial anesthesia, the discharge of the rat ventral oblique muscle was recorded at CRD pressures of 40 and 60 mmHg. EMG responses to different degrees of CRD were recorded using the RM6240BD system (Chengdu, China). Data were analyzed by averaging the amplitude of the baseline. Values over the baseline were used to assess visceral hypersensitivity[21].

Morris water maze (MWM)

The MWM consisted of a circular tank circled by dark curtains and was used to assess hippocampal-dependent spatial learning and memory. The water was made opaque by adding the prepared Chinese ink and was separated into four equal quadrants. The first day of water maze training was dedicated to adapting the rats to the aquatic labyrinth. In the center of the fourth quadrant, there was a hidden platform located 1 cm below the water surface. The trials were performed four times per day for a total of six days and the latency of the rats finding the platform was recorded[22]. The body trajectories of the rats were recorded using an animal visual tracking system (YiShu, Shanghai).

Protein extraction and western blot

The RIPA buffer came from Millipore. Protease inhibitor (PMSF) were from Sigma. Protein from the hippocampus of rats were extracted by RIPA and PMSF, separated via 8% SDS-PAGE, and electro-transferred onto PVDF (Invitrogen, USA) membranes, which were probed with rabbit anti-enhancer of zeste homolog 2 (EZH2) (5246S,1:1000, Cell Signaling Technology [CST], USA), rabbit anti-EED (85322,1:1000, CST, USA) rabbit anti-SUZ12 (3737,1:1000, CST, USA), and mouse anti-β-actin primary antibody (8226,1:1000, Abcam, USA). Furthermore, the expression of protein levels and quantification of IF were detected using ImageJ (http://rsb.info.nih.gov/ij/).

RNA extraction and quantitative real-time PCR (qPCR)

Total RNA was extracted using TRIzol (Invitrogen, USA). An Evo-M-MLV reverse transcription kit (Accurate Biology, China) was used to perform reverse transcription for circRNA and mRNA, according to the manufacturer's instructions. The miRNA 1st-strand cDNA synthesis kit (Accurate Biology, China) was used to perform reverse transcription for microRNA, according to the manufacturer's instructions. Nuclear and cytosolic fractions of cells were purified using a nuclear/cytosolic fractionation kit (AM1921 Thermo Fisher), as per the manufacturer's instructions. After reverse transcription, qRT-PCR was conducted according to the manufacturer's instructions. Primer sequences were shown in Table 1.

Table 1
Primer used qRT-PCR detection

gene	primer	Sequence (5'-3')
CIRCKcnk9	Forward	AAAACCACAGGCTGCACATC
	Reverse	CATAACCAGCGTCAGAGGGA
circStk39	Forward	GTGAGAGGCTATGACTTCAA
	Reverse	GCAGATAGTCTAATCCTTCC
circRab30	Forward	CCAACAGAGAGCAGAAGAGT
	Reverse	GGAGCGAAATCTCTCTTGAC
CircQrich1	Forward	ACATGAAGTTCTGAAGGACG
	Reverse	GTACTCTTCAAATGAGATGG
circCept1	Forward	GAAGAGTACCCTCATGGATT
	Reverse	GTTTCCTTGTTGACCGATGC
circTtll5	Forward	GTGAGTTGTGATGATCCAGA
	Reverse	GTAACGGGAGACCAAGATGT
circAff4	Forward	CATGGAGGATCTCATCAGAG
	Reverse	CTGAATTTCCTGATTCCGCC
circZfp827	Forward	CCAGTCTGTCATTTTCCCCA
	Reverse	CTTGACACTGCAGTGAGTCT
mkcnk9	Forward	CGCAAGTCCATCTAAGTGTG
	Reverse	GCATAGAACATACAGAAGGCC
mEZH2	Forward	TAAGGGCACA
	Reverse	TACATTCAGG
U6	Forward	GGAACGATACAGAGAAGATTAGC
	Reverse	TGGAACGCTTCACGAATTTGCG
GAPDH	Forward	ACTCCCATTCTTCCACCTTTG
	Reverse	CCCTGTTGCTGTAGCCATATT
miR-124-3p		AGTGCAGGGTCCGAGGTATT

RNA immunoprecipitation (RIP)

The hippocampus were fragmented by ultrasound. RNA immunoprecipitation was performed using the RIP RNA-Binding Protein Immunoprecipitation Kit (BersinBio Biotech., Guangzhou, Guangdong, China)[23] with anti-AGO2 (#2897, 1:150, CST, USA) and anti-EZH2 (5246S, 1:50, CST, USA). The input was set as a positive control, and IgG was used as a negative control. Coprecipitated circKcnk9 and miR-124-3p levels were evaluated by qPCR.

Luciferase reporter assay

PC12 cells were cultured in DMEM containing 5% FBS (Thermo, USA) and 1% penicillin/streptomycin, and were transfected with mimic124-3p/ nc at a concentration of 50nM oligonucleotides using Lipofectamine 3000 (Invitrogen), according to the manufacturer's protocol. For the luciferase reporter assay, pmirGLO dual-luciferase vectors (GenePharma, shanghai) were used to construct dual-luciferase reporter plasmids. Sequences of miR-124-3p and circKcnk9 were separately cloned into vectors (Fig.S2). PC12 cells were co-transfected with wild-type pmirGLO-circKcnk9 or the mutated type and miR-124 mimics (negative control). After induction for 48 h, luciferase activity was assessed using a dual-luciferase reporter kit (Promega, Madison, WI, USA). GloMax® 20/ 20 system (Promega,USA) was used to test the luciferase activity. Relative firefly luciferase activity was normalized to Renilla luciferase activity.

RNA fluorescent in situ hybridization

Rats were deeply anesthetized with Ulatan (0.5 mL/ 100g) and perfused transcardially with 500 mL ice-cold 0.9% NaCl, followed by 750 mL 4% paraformaldehyde. The brains were removed from the skull and placed in formalin overnight. After gradient dehydration with 20% and 30% sucrose (Sigma, USA), tissues were embedded with OCT compound and sectioned using a cryotome (Lecia, Germany). RNA localization and quantification were determined using a FISH kit from GenePharma (Shanghai, China) and RNA probe from Exiqon (Exiqon Life Sciences, Denmark), according to the manufacturer's protocol. For combined RNA FISH and immunostaining, we performed RNA FISH first, followed by immunofluorescence. Diethyl pyrocarbonate-treated water was used in all steps to rule out RNA degradation.

Immunofluorescence

Removed the sections (20–40μm) from − 20℃ refrigerator for half an hour before using. We used PBS (phosphate buffer solutionc) to wash out OCT. Pap Pen was used to circle out the tissue. The sections were blocked with immunostaining blocking buffer solution containing 5% goat serum and 0.3% Triton^{TM}X-100 at room temperature for 2 hours (or 37℃ for 30min), and then incubated with primary antibodies at 4℃ for 24–48 hours. Sections were incubated with secondary antibodies at room temperature for 2 h before washing out with PBS (3times/ 15min). Imunofluorescence of frozen sections was performed using the primary antibodies described below Table 2.

Table 2
Primary antibodies

antibodies	Art.No	ratio
EZH2	CST 5246S	1:100
GFAP	CST 3670S	1:300
NEUN	Millipore MAB377	1:300
IBA-1	Woko PTR2404	1:5000
DAPI	Beyotime C1002	1:1000

Secondary antibodies: Goat anti-Rabbit lgG, 488 (150073, 1:300, Abcam); Goat anti-Mouse lgG, 488 (150105, 1:300, Abcam); Goat anti-Rabbit lgG 594 (8889S, 1:500, CST); Goat anti-Mouse lgG, 594 (150108, 1:300, Abcam).

Immunofluorescence and FISH images were captured using Lecia SP5 confocal microscopes equipped with 405, 488, and 594 lasers. The contrast of the final images were adjusted using Photoshop (Adobe Systems, Mountain View, CA, USA).

Bioinformatic analysis

Delineation of circRNA/miRNA interactions was predicted using miRanda (http://www.microrna.org/microrna/home.do). Circular plots of circRNA-miRNA-binding sites were plotted using (http://www.bioinformatics.com.cn) a free online platform for data analysis and visualization. Venn diagrams were created using the Lianchuan Cloud platform (Hangzhou Lianchuan Biotechnology Co. Ltd., Hangzhou, China). A PPI network of the HUB gene was obtained using the STRING database (https://string-db.org) and visualized using Cytoscape[24].

Slice preparation and field potential recording

Rats (6–8 weeks) were anesthetized with isoflurane (2%) and the brain was removed out rapidly by decapitation. Acute coronal slices (400 μm thick) including the hippocampus were obtained using a vibrating-knife microtome (Leica VT1000s) in oxygenated, ice-cold, high-sucrose cutting solution (Sigma, USA). The coronal hippocampal slices were rapidly removed and transferred to 30°C, oxygenated (95% O_2, 5% CO_2 pH 7.4) artificial cerebrospinal fluid (ACSF). The slices were incubated in an interface recording chamber maintained at a constant temperature and allowed to equilibrate for at least 1.5 h. Each brain slice was recorded only once.

For recording, the hippocampal slices were transferred to a chamber, submerged, and superfused continuously with ACSF at a flow rate of 1–2 mL/min for recording at room temperature (23°C ± 2°C). The Schaffer collaterals were stimulated and fEPSPs were recorded from the dendritic layer of the CA1 pyramidal cells, as reported by Kleppisch et al for local field potential recordings in the hippocampus[25],

brain slices were stabilized by electrode single stimulation for 10 min. LTP was then induced by two episodes of high-frequency stimulation at 10-s intervals.

Statistical analysis

All data were presented as mean ± standard error of the mean. In behavioral tests and molecular biology experiments, two-tailed independent sample t-tests were performed to determine differences between control and IBS-like rats if data satisfied the normal distribution, and if data did not satisfy normal distribution, Wilcoxon correction was performed for two independent samples. Statistical analysis of data from more than two groups was performed using one-way analysis of variance (ANOVA)-LSD-t comparisons if the data were normally distributed. The rank sum test, Kruskal–Wallis H test, and Nemenyi test were performed when the data did not satisfy normal distribution and were more than two groups. In addition, repeated-measures ANOVA was performed to analyze the electrophysiological results. The EMG results were analyzed using a two-way ANOVA. Correlation analysis was performed using a two-tailed Pearson correlation. The data analysis was performed using GraphPad Prism8 and R4.0.3, and a *P*-value of < 0.05 was considered statistically significant.

Results

Neonatal CRD induces visceral hypersensitivity and anxiety in rats

The IBS-like model was established using neonatal CRD (Fig. 1A). Visceral sensitivity was assessed by recording the response of EMG to CRD (Fig. 1B and C). The amplitudes of EMG at 40 and 60 mmHg both increased significantly in IBS-like rats compared to those in controls, indicating that IBS-like rats experience visceral hypersensitivity. Since patients with IBS are often comorbid with anxiety, we examined anxiety-related behaviors using OFT and EPM. OFT results showed the time and distance in the center area decreased significantly (Fig. 1D-G) without difference in the total distance in IBS-like rats (Fig. 1E). Anxiety-like behaviors of IBS-like rats were also observed in the EPM where the percentage of entries, time and distance into the open arms decreased significantly (Fig. 1H–K). Then we used MWM to test whether chronic visceral pain and negative emotion affect cognitive ability. We found there was no significant difference in escape latency, path length and time of the target quadrant, and number passing the platform between control and IBS-like rats (Fig. 1L–P). Taken all, IBS-like rats show visceral hypersensitivity and co-morbid anxiety without cognitive impairment.

Increased CA1 circKcnk9 is involved in visceral hypersensitivity and anxiety comorbid by enhancing LTP in IBS-like rats

First, we used qPCR to examine the expressions of pain-related circular RNAs in the hippocampus and found a significant increase in circKcnk9 expression (Fig. 2A) in IBS-like rats. Next, distribution of circKcnk9 was determined by FISH experiments. We found circKcnk9 was high expressed in the hippocampus of IBS-like rats (Fig. 2B). The CA1 region was selected as the quantification zone (Fig. 2C)

and RNA FISH showed the number of circKcnk9^{+} cells was higher in IBS-like rats than in controls (Fig. 2D). Furthermore, circKcnk9 was largely colocalized with neurons but not with microglia or astrocytes (Fig. 2G).

Since the expression of CA1 circKcnk9 increased in IBS-like rats, we observed the effects of intervening CA1 circKcnk9 expression level on LTP, visceral pain and anxiety in rats. Adeno-associated virus (AAV) was microinjected into CA1 of control rats to overexpress circKcnk9 while shcircKcnk9 was microinjected into CA1 of IBS-like rats to knockdown circKcnk9. IF and qPCR confirmed that the circKcnk9 AAV/shRNA virus was successfully expressed in the hippocampus (Fig. 2E and F). Field potential experiments found overexpression of circKcnk9 enhanced CA1 LTP in the hippocampal slices of control rats, whereas circKcnk9 knockdown attenuated CA1 LTP in IBS-like rats (Fig. 3A and B). Compared with the controls with empty-loaded virus, the control rats that overexpressed circKcnk9 traveled less time and distance in the central area of the OFT (Fig. 3C-E) and had a decreased percentage of distance, time, and entries in the open arm of the EPM (Fig. 3F-H). The EMG results showed that overexpression of circKcnk9 induced visceral hypersensitivity in controls (Fig. 3I &J). In contrast, IBS-like rats with CA1 shcircKcnk9 showed an increase in the central distance and time in the OFT (Fig. 3C-E) and had an increased percentage of distance, time, and entries in the open arm of the EPM (Fig. 3F-H). The EMG results also showed that CA1 shcircKcnk9 treatment alleviated visceral hypersensitivity in IBS-like rats (Fig. 3I and J).

Taken all together, increased circKcnk9 is expressed in CA1 of IBS-like rats and CA1 shcircKcnk9 treatment inhibits LTP and alleviates visceral hypersensitivity and anxiety in IBS-like rats. On the other hand, overexpression of CA1 circKcnk9 enhances LTP and induces visceral hypersensitivity and anxiety in control rats. Accordingly, we infer that increased CA1 circKcnk9 expression induced by early life stress regulates visceral pain and anxiety though enhancing LTP in IBS-like rats.

CircKcnk9 acts as a miR-124-3p sponge to regulate LTP, visceral hypersensitiviry and anxiety comorbidity in CA1 of rats

Literatures have been reported that circRNAs can act as miRNA sponges to modulate the expression of target genes[26, 27]. Then we used MiRanda database to predict the binding sites and found circKcnk9 has three binding sites for miR-124-3p (Fig. 4A). The dual-luciferase reporter assay suggested circKcnk9 can directly adsorb miR-124-3p through three predicted sites (Fig. 4B). The confocal images confirmed the colocalization of circKcnk9 with miR-124-3p (Fig. 4C). The RIP assay showed circKcnk9 coprecipitated with miR-124-3p by AGO2, the vital component of the RNA-induced silencing complex, indicating circKcnk9 acts as a miR-124-3p sponge (Fig. 4D). qPCR showed hippocampal miR-124-3p expression decreased in IBS-like rats (Fig. 4E). In addition, qPCR suggested CA1 circKcnk9 overexpression reduced the expression of miR-124-3p in control rats (Fig. 4F), whereas CA1 shcircKcnk9 treatment increased miR-124-3p expression in IBS-like rats (Fig. 4G), indicating there is a negative correlation between circKcnk9 and miR-124-3p which was further confirmed by correlation analysis (Fig. 4H).

As the expression of CA1 miR-124-3p decreased in IBS-like rats, we observed the influence of modifying CA1 miR-124-3p expression on LTP, visceral pain and anxiety in rats. AntagomiR-124-3p was microinjected into CA1 of control rats to inhibit the expression of miR-124-3p while agomiR-124-3p was microinjected into CA1 of IBS-like rats to increase the expression of miR-124-3p. Field potential experiments showed inhibiting miR-124-3p enhanced CA1 LTP in the hippocampal slices of control rats, whereas increasing miR-124-3p attenuated CA1 LTP in IBS-like rats (Fig. 5A and B). Compared with antagonc, the control rats treated with antagomiR-124-3p in the CA1traveled less time and distance in the central area of the OFT (Fig. 5C-E) and had a decreased percentage of distance, time, and entries in the open arm of the EPM (Fig. 5F-H). The EMG results showed that inhibiting miR-124-3p induced visceral hypersensitivity in controls (Fig. 5I and J). In contrast, IBS-like rats with CA1 administration of agomiR-124-3p showed an increase in the central distance and time in the OFT (Fig. 5C-E) and had an increased percentage of distance, time, and entries in the open arm of the EPM (Fig. 5F-H). The EMG results also showed that CA1 treatment of agomiR-124-3p alleviated visceral hypersensitivity in IBS-like rats (Fig. 5I and J). The results point toward that increased CA1 circKcnk9 acts as miR-124-3p sponge, which results in the inhibiting effect of miR-124-3p on gene silencing to cause enhanced LTP, visceral hypersensitiviry and anxiety in IBS-like rats.

EZH2 is a target gene of CircKcnk9/miR-124-3p and affects the visceral hypersensitiviry and anxiety of IBS-like rats by modifying CA1 LTP

Because a single miRNA has the potential to regulate hundreds of transcripts, we predicted putative targets for miR-124-3p using five databases: PITA, TargetScan, microT, miwalk, and Pictar (Fig. 6A). We used the MCODE algorithm for multiple target genes of miR-124-3p and screened the HUB genes (Fig. 6B). Then EZH2 was selected as a target gene of miR-124-3p in IBS-like rat because EZH2 is associated with anxiety and pain. Bioinformatics analysis showed the binding sequence of EZH2 with miR124-3p is high conservative in Human, mouse and rat (Fig. 6C). Western blots showed a significant increase in CA1 EZH2 expression in IBS-like rats (Fig. 6D). Furthermore, the expression of EZH2 decreased after administration of agomiR-124-3p in IBS-like rats (Fig. 6E) while the expression of EZH2 was increased after antagomiR-124-3p administration in controls (Fig. 6F), indicating miR-124-3p could inhibit EZH2 expression in the hippocampus. Furthermore, we speculated CA1 EZH2 expression should be regulated by circKcnk9 due to our finding that increased CA1 circKcnk9 acts as miR-124-3p sponge in IBS-like rats. Therefore, we examined the protein expression of EZH2 after intervening the level of circKcnk9. Overexpression of CA1 circKcnk9 increased the protein level of EZH2 in control rats (Fig. 6G), whereas CA1 shcircKcnk9 decreased the protein level of EZH2 in IBS-like rats (Fig. 6H).

In the light of our finding that CA1 EZH2 expression was increased in IBS-like rats, we microinjected siEZH2 into CA1 to knock down EZH2 and consequently examined its effects on visceral hypersensitivity, anxiety and CA1 LTP. Western blots confirmed CA1 EZH2 expression decreased after CA1 treatment of siEZH2 in IBS-like rats (Fig. 7A). IBS-like rats with CA1 treatment of siEZH2 showed an increase in the central distance and time in the OFT (Fig. 7B-D) and had an increased percentage of distance, time, and entries in the open arm of the EPM (Fig. 7E-G). The EMG results also showed that CA1 administration of

siEZH2 alleviated visceral hypersensitivity in IBS-like rats (Fig. 7H). In addition, CA1 treatment of siEZH2 attenuated CA1 LTP in the hippocampal slices of IBS-like rats (Fig. 7I). Those results suggest EZH2 is a target gene of miR-124-3p and increased EZH2 expression is involved in visceral hypersensitivity and anxiety of IBS-like rats by regulating synaptic plasticity.

Discussion

In this study, we have explored an epigenetic molecular mechanism underlying visceral hypersensitivity and anxiety comorbidity in IBS-like rats. Neonatal CRD induced visceral hypersensitivity and anxiety of IBS-like rats. The expression of hippocampal circKcnk9, a novel circRNA we identified, was increased significantly in IBS-like rats. CA1 shcircKcnk9 treatment inhibited LTP and alleviated visceral hypersensitivity and anxiety in IBS-like rats while overexpression of CA1 circKcnk9 enhanced LTP and induced visceral hypersensitivity and anxiety in control rats. Several lines of experiments indicate increased CA1 circKcnk9 acts as miR-124-3p sponge, resulting in the inhibition of miR-124-3p role in gene silencing to cause enhanced LTP, visceral hypersensitiviry and anxiety in IBS-like rats. CA1 administration of agomiR-124-3p decreased CA1 LTP amplitude, visceral pain response and anxiety in IBS-like rats. In contrast, CA1 treatment with antagomiR-124-3p induced LTP, visceral hypersensitivity and anxiety in control rats. Furthermore, bioinformatics analysis and experimental data showed EZH2 is a target gene of miR-124-3p and increased EZH2 expression is involved in visceral hypersensitivity and anxiety of IBS-like rats by regulating synaptic plasticity.

In the current study, neonatal CRD induced visceral hypersensitivity and anxiety comorbidity of IBS-like rats. Our previous study demonstrated that long-term potentiation (LTP) is enhanced in the hippocampal CA1 of IBS-like rats[12]. As one model of early life stress, neonatal CRD may induce abnormal synaptic plasticity and adverse memory in the hippocampus which is at least in part responsible for visceral hypersensitivity and anxiety comorbidity of IBS-like rats.

Chronic phenotypes are often associated with epigenetic modulation of gene expression. In the light of the literatures that hippocampal circRNAs may be involved in the regulation of pain[8], negative emotions[9] and synaptic plasticity[15], we compared the differential expression of several circRNAs in the hippocampal CA1 between IBS-like rats and controls. Interesting, we found CA1 circKcnk9 was increased significantly in IBS-like rats. And circKcnk9 was largely colocalized with neurons but not microglia or astrocytes, which is supported by the studies that circRNAs are abundantly expressed in neurons[28, 29]. Different circRNAs may play different roles in chronic pain and negative emotions. For example, circ-Ankib1 and circAnks1a are involved in the development of neuropathic pain[10]; circRNA_104670 and circSEMA4B are involved in low back pain[30]; circSlc7a11 overexpression is involved in bone cancer pain[31]; circSTAG1 was significantly decreased in the hippocampus of chronic unpredictable stress-treated mouse and in peripheral blood of patients with major depressive disorder[9]. These studies indicate the roles of different circRNAs seem relatively specific, which could be used for disease diagnosis and treatment. However, the role of circKcnk9 has not been reported in other disorders.

Due to increased expression of CA1 circKcnk9 in IBS-like rats, we hypothesized intervening the expression level of CA1 circKcnk9 could regulate LTP, visceral pain and anxiety in rats. In support, adeno-associated virus (AAV) was microinjected into CA1 of control rats to overexpress circKcnk9 while shcircKcnk9 was microinjected into CA1 of IBS-like rats to knockdown circKcnk9. As expected, overexpression of hippocampal circKcnk9 induced visceral hypersensitivity and anxiety in controls while knockdown of circkcnk9 attenuated visceral hypersensitivity and anxiety in IBS-like rats. The behavioral evidence supported our finding that CA1 circKcnk9 is a key molecule for visceral hypersensitivity and anxiety comorbidity of IBS-like rats. In line with behavior results, electrophysiological experiments revealed overexpression of CA1 circKcnk9 facilitated high frequency-induced LTP in controls, whereas knockdown of circkcnk9 inhibited LTP in IBS-like rats, indicating circKcnk9 could affect synaptic plasticity and cause central sensitivity. It was reported neural circRNAs are derived from synaptic genes and regulated by development and plasticity[29], which was consistent with our findings. Combined together, our results suggest that neonatal CRD stress induces increased CA1 circKcnk9 expression, which leads to visceral hypersensitivity and anxiety comorbidity though regulating synaptic plasticity in IBS-like rats.

Literatures have been reported that circRNAs can act as miRNA sponges to modulate the expression of target genes[16]. Chronic pain related studies found that miR-124-3p is involved in neuropathic pain of CCI rat models[32, 33]. In addition, mice exposed to chronic ultra-mild stress exhibited increased depression-like behaviors and reduced hippocampal expression of the brain-enriched miR-124[18]. In our results, increased CA1 circKcnk9 expression leads to visceral hypersensitivity and anxiety comorbidity of IBS-like rats. We next sought to explore the mechanism underlying CA1 circKcnk9 role in IBS-like rats. The confocal images and RIP assay confirmed that circKcnk9 is colocalized with miR-124-3p and acts as a miR-124-3p sponge. Furthermore, MiRanda database and dual-luciferase reporter assay suggested circKcnk9 can directly adsorb miR-124-3p through three predicted sites. Meanwhile, qPCR quantification showed hippocampal miR-124-3p expression decreased in IBS-like rats. Since circKcnk9 acts as a miR-124-3p sponge and a negative correlation between circKcnk9 and miR-124-3p. It is conceivable that gene regulation of CA1 miR-124-3p will have opposite effects on CA1 LTP and behaviors of rats. This speculation was confirmed by the electrophysiological and behavioral experiments that CA1 miR-124-3p upregulation decreased CA1 LTP amplitude, visceral hypersensitivity and anxiety in IBS-like rats while miR-124-3p downregulation induced LTP, visceral hypersensitivity and anxiety in control rats. Intrahippocampal supplementation with miR-124-3p could be a novel therapy for IBS, which was also studied in epilepsy[34].

MicroRNAs are important post-transcriptional regulators of gene expression that act by direct base pairing to target sites within untranslated regions of mRNAs. Literatures reported that miR-124-3p/EZH2 signaling pathway was involved in cancer[35–37]. MiR-124-3p was also found significantly downregulated in rats after chronic sciatic nerve injury and its direct target gene was EZH2[32]. To explore whether EZH2 is a target gene of circKcnk9/miR-124-3p in hippocampus of IBS-like rats, we designed a battery of experiments to clarify the molecular mechanism. We screened out EZH2 through bioinformatics analysis and confirmed that EZH2 is one of the target genes for miR-124-3p and the binding sequence of EZH2 with miR-124-3p is high conservative in Human, mouse and rat. Moreover,

western blots showed a significant increase in CA1 EZH2 expression in IBS-like rats. Furthermore, the expression of EZH2 decreased after upregulation of miR-124-3p or downregulation of circKcnk9 in the CA1 of IBS-like rats. Then through the stereotaxic administration of siEZH2 into CA1 to knock down EZH2 and consequently examined its effects on visceral hypersensitivity, anxiety and CA1 LTP. Certainly, CA1 treatment with siEZH2 downregulated CA1 LTP, visceral hypersensitivity and anxiety in IBS-like rats. EZH2 is a target gene of not only miR-124-3p but also other miRNAs[38–40]. It is reasonable to consider that EZH2 is the common cellular pathway involved in many disorders including cancer[41], chronic pain[42] and negative emotions[43, 44].

In conclusion, the most important finding in the study is that early life stress induces increased expression of circKcnk9, a novel circRNA, in the CA1 of IBS-like rats. Increased circKcnk9 ensuing regulates the synaptic transmission and enhances LTP, leading to visceral hypersensitivity and anxiety comorbidity in IBS-like rats. The underlying signaling pathway of circKcnk9 is miR-124-3p/EZH2. Increased circKcnk9 reinforces its sponge for miR-124-3p, strongly suppresses miR-124-3p action, resulting in increased expression of target gene EZH2. The study provides a new epigenetic mechanism of visceral hypersensitivity and anxiety comorbidity in IBS-like rats and circKcnk9 may be a key molecule for the treatment of IBS.

Declarations

Acknowledgements We thank the Public Technology Service Center of Fujian Medical University (China) for providing technical support and experimental platforms.

Author contributions Y.L. wrote the first draft and designed the research; Y.L., Z.-H. L, and Y.-F. Z. performed the experiments; Y.C, Z.C, Y.-F. Z and B.W contributed to the acquisition of data; Y.L. performed the bioinformatic analysis. B.W, Z.C., and Y.-F.Z. analyzed the data. Y L, W L, C.L. and A-Q. C. wrote and revised the manuscript.

Funding We would like to thank the Foundation of Science and Technology of Fujian Province (2018Y9069), Natural Science Foundation of Fujian Province (2021J01675, 2020J01608), the funders played no role in the study design or implementation.

Data Availability The datasets used or analyzed during the current study are available from the corresponding author on reasonable request.

Ethics Approval All experimental procedures were conducted according to the guidelines for animal experimentation of the Fujian medical University and animal experiments were approved by the local ethics committee (under grant IACUC FJMU 2022-NSFC-0273).

Consent to Participate Not applicable.

Consent for Publication All authors whose names appear on the submission agreed to the version to be published.

Competing Interests The authors declare no competing interests.

References

1. Yu V, Ballou S, Hassan R, Singh P, Shah E, Rangan V et al (2021) Abdominal Pain and Depression, Not Bowel Habits, Predict Health Care Utilization in Patients With Functional Bowel Disorders. Am J Gastroenterol 116(8):1720–1726. doi: 10.14309/ajg.0000000000001306
2. Midenfjord I, Borg A, Törnblom H, Simrén M (2021) Cumulative Effect of Psychological Alterations on Gastrointestinal Symptom Severity in Irritable Bowel Syndrome. Am J Gastroenterol 116(4):769–779. doi: 10.14309/ajg.0000000000001038
3. Black CJ, Yiannakou Y, Guthrie EA, West R, Houghton LA, Ford AC (2021) A Novel Method to Classify and Subgroup Patients With IBS Based on Gastrointestinal Symptoms and Psychological Profiles. Am J Gastroenterol 116(2):372–381. doi: 10.14309/ajg.0000000000000975
4. O'Mahony SM, Clarke G, Dinan TG, Cryan JF (2017) Irritable Bowel Syndrome and Stress-Related Psychiatric Co-morbidities: Focus on Early Life Stress. Handb Exp Pharmacol 239:219–246. doi: 10.1007/164_2016_128
5. Louwies T, Ligon CO, Johnson AC, Greenwood-Van Meerveld B (2019) Targeting epigenetic mechanisms for chronic visceral pain: A valid approach for the development of novel therapeutics. Neurogastroenterology and motility: the official journal of the European Gastrointestinal Motility Society 31(3):e13500. doi: 10.1111/nmo.13500
6. Chen Q, Wang H, Li Z, Li F, Liang L, Zou Y et al (2022) Circular RNA ACTN4 promotes intrahepatic cholangiocarcinoma progression by recruiting YBX1 to initiate FZD7 transcription. J Hepatol 76(1):135–147. doi: 10.1016/j.jhep.2021.08.027
7. Gao X, Xia X, Li F, Zhang M, Zhou H, Wu X et al (2021) Circular RNA-encoded oncogenic E-cadherin variant promotes glioblastoma tumorigenicity through activation of EGFR-STAT3 signalling. Nat Cell Biol 23(3):278–291. doi: 10.1038/s41556-021-00639-4
8. Zheng YL, Guo JB, Song G, Yang Z, Su X, Chen PJ et al (2022) The role of circular RNAs in neuropathic pain. Neurosci Biobehav Rev 132:968–975. doi: 10.1016/j.neubiorev.2021.10.048
9. Huang R, Zhang Y, Bai Y, Han B, Ju M, Chen B et al (2020) N(6)-Methyladenosine Modification of Fatty Acid Amide Hydrolase Messenger RNA in Circular RNA STAG1-Regulated Astrocyte Dysfunction and Depressive-like Behaviors. Biol Psychiatry 88(5):392–404. doi: 10.1016/j.biopsych.2020.02.018
10. Zhang SB, Lin SY, Liu M, Liu CC, Ding HH, Sun Y et al (2019) CircAnks1a in the spinal cord regulates hypersensitivity in a rodent model of neuropathic pain. Nat Commun 10(1):4119. doi: 10.1038/s41467-019-12049-0
11. Zhang Y, Zhang X, Xing Z, Tang S, Chen H, Zhang Z et al (2020) circStrn3 is involved in bone cancer pain regulation in a rat model. Acta Biochim Biophys Sin 52(5):495–505. doi: 10.1093/abbs/gmaa018

12. Chen Y, Chen AQ, Luo XQ, Guo LX, Tang Y, Bao CJ et al (2014) Hippocampal NR2B-containing NMDA receptors enhance long-term potentiation in rats with chronic visceral pain. Brain Res 1570:43–53. doi: 10.1016/j.brainres.2014.05.001
13. Ren LY, Meyer MAA, Grayson VS, Gao P, Guedea AL, Radulovic J (2022) Stress-induced generalization of negative memories is mediated by an extended hippocampal circuit. Neuropsychopharmacology: official publication of the American College of Neuropsychopharmacology 47(2):516–523. doi: 10.1038/s41386-021-01174-4
14. Mao J, Li T, Fan D, Zhou H, Feng J, Liu L et al (2020) Abnormal expression of rno_circRNA_014900 and rno_circRNA_005442 induced by ketamine in the rat hippocampus. BMC Psychiatry 20(1):1. doi: 10.1186/s12888-019-2374-2
15. Xu K, Zhang Y, Xiong W, Zhang Z, Wang Z, Lv L et al (2020) CircGRIA1 shows an age-related increase in male macaque brain and regulates synaptic plasticity and synaptogenesis. Nat Commun 11(1):3594. doi: 10.1038/s41467-020-17435-7
16. Zeng Z, Xia L, Fan S, Zheng J, Qin J, Fan X et al (2021) Circular RNA CircMAP3K5 Acts as a MicroRNA-22-3p Sponge to Promote Resolution of Intimal Hyperplasia Via TET2-Mediated Smooth Muscle Cell Differentiation. Circulation 143(4):354–371. doi: 10.1161/circulationaha.120.049715
17. Dube U, Del-Aguila JL, Li Z, Budde JP, Jiang S, Hsu S et al (2019) An atlas of cortical circular RNA expression in Alzheimer disease brains demonstrates clinical and pathological associations. Nat Neurosci 22(11):1903–1912. doi: 10.1038/s41593-019-0501-5
18. Higuchi F, Uchida S, Yamagata H, Abe-Higuchi N, Hobara T, Hara K et al (2016) Hippocampal MicroRNA-124 Enhances Chronic Stress Resilience in Mice. J neuroscience: official J Soc Neurosci 36(27):7253–7267. doi: 10.1523/jneurosci.0319-16.2016
19. Grace PM, Strand KA, Galer EL, Maier SF, Watkins LR (2018) MicroRNA-124 and microRNA-146a both attenuate persistent neuropathic pain induced by morphine in male rats. Brain Res 1692:9–11. doi: 10.1016/j.brainres.2018.04.038
20. Al-Chaer ED, Kawasaki M, Pasricha PJ (2000) A new model of chronic visceral hypersensitivity in adult rats induced by colon irritation during postnatal development. Gastroenterology 119(5):1276–1285. doi: 10.1053/gast.2000.19576
21. Fan F, Tang Y, Dai H, Cao Y, Sun P, Chen Y et al (2020) Blockade of BDNF signalling attenuates chronic visceral hypersensitivity in an IBS-like rat model. Eur J Pain 24(4):839–850. doi: 10.1002/ejp.1534
22. Levit A, Gibson A, Hough O, Jung Y, Agca Y, Agca C et al (2021) Precocious White Matter Inflammation and Behavioural Inflexibility Precede Learning and Memory Impairment in the TgAPP21 Rat Model of Alzheimer Disease. Mol Neurobiol 58(10):5014–5030. doi: 10.1007/s12035-021-02476-w
23. Ma S, Gu X, Shen L, Chen Y, Qian C, Shen X et al (2021) CircHAS2 promotes the proliferation, migration, and invasion of gastric cancer cells by regulating PPM1E mediated by hsa-miR-944. Cell Death Dis 12(10):863. doi: 10.1038/s41419-021-04158-w

24. Shannon P, Markiel A, Ozier O, Baliga NS, Wang JT, Ramage D et al (2003) Cytoscape: a software environment for integrated models of biomolecular interaction networks. Genome Res 13(11):2498–2504. doi: 10.1101/gr.1239303
25. Kleppisch T, Pfeifer A, Klatt P, Ruth P, Montkowski A, Fässler R et al (1999) Long-term potentiation in the hippocampal CA1 region of mice lacking cGMP-dependent kinases is normal and susceptible to inhibition of nitric oxide synthase. J neuroscience: official J Soc Neurosci 19(1):48–55. doi: 10.1523/jneurosci.19-01-00048.1999
26. van Zonneveld AJ, Kölling M, Bijkerk R, Lorenzen JM (2021) Circular RNAs in kidney disease and cancer. Nat Rev Nephrol 17(12):814–826. doi: 10.1038/s41581-021-00465-9
27. Kristensen LS, Andersen MS, Stagsted LVW, Ebbesen KK, Hansen TB, Kjems J (2019) The biogenesis, biology and characterization of circular RNAs. Nat Rev Genet 20(11):675–691. doi: 10.1038/s41576-019-0158-7
28. Knupp D, Cooper DA, Saito Y, Darnell RB, Miura P (2021) NOVA2 regulates neural circRNA biogenesis. Nucleic Acids Res 49(12):6849–6862. doi: 10.1093/nar/gkab523
29. You X, Vlatkovic I, Babic A, Will T, Epstein I, Tushev G et al (2015) Neural circular RNAs are derived from synaptic genes and regulated by development and plasticity. Nat Neurosci 18(4):603–610. doi: 10.1038/nn.3975
30. Lin Z, Lu F, Ma X, Xia X, Zou F, Jiang J (2021) Roles of circular RNAs in the pathogenesis of intervertebral disc degeneration (Review). Experimental and therapeutic medicine 22(5):1221. doi: 10.3892/etm.2021.10655
31. Chen HW, Zhang XX, Peng ZD, Xing ZM, Zhang YW, Li YL (2021) The circular RNA circSlc7a11 promotes bone cancer pain pathogenesis in rats by modulating LLC-WRC 256 cell proliferation and apoptosis. Mol Cell Biochem 476(4):1751–1763. doi: 10.1007/s11010-020-04020-1
32. Zhang Y, Liu HL, An LJ, Li L, Wei M, Ge DJ et al (2019) miR-124-3p attenuates neuropathic pain induced by chronic sciatic nerve injury in rats via targeting EZH2. J Cell Biochem 120(4):5747–5755. doi: 10.1002/jcb.27861
33. Wei M, Li L, Zhang Y, Zhang M, Su Z (2020) Downregulated circular RNA zRANB1 mediates Wnt5a/β-Catenin signaling to promote neuropathic pain via miR-24-3p/LPAR3 axis in CCI rat models. Gene 761:145038. doi: 10.1016/j.gene.2020.145038
34. Wang W, Wang X, Chen L, Zhang Y, Xu Z, Liu J et al (2016) The microRNA miR-124 suppresses seizure activity and regulates CREB1 activity. Expert Rev Mol Med 18:e4. doi: 10.1017/erm.2016.3
35. Zhu B, Cui H, Xu W (2021) Hydrogen inhibits the proliferation and migration of gastric cancer cells by modulating lncRNA MALAT1/miR-124-3p/EZH2 axis. Cancer Cell Int 21(1):70. doi: 10.1186/s12935-020-01743-5
36. Yang X, Wang J, Li H, Sun Y, Tong X (2021) Downregulation of hsa_circ_0026123 suppresses ovarian cancer cell metastasis and proliferation through the miR–124–3p/EZH2 signaling pathway. Int J Mol Med 47(2):668–676. doi: 10.3892/ijmm.2020.4804

37. Sha J, Xia L, Han Q, Chi C, Zhu Y, Pan J et al (2020) Downregulation of circ-TRPS1 suppressed prostatic cancer prognoses by regulating miR-124-3p/EZH2 axis-mediated stemness. Am J cancer Res 10(12):4372–4385
38. Gao P, Zeng X, Zhang L, Wang L, Shen LL, Hou YY et al (2021) Overexpression of miR-378 Alleviates Chronic Sciatic Nerve Injury by Targeting EZH2. Neurochem Res 46(12):3213–3221. doi: 10.1007/s11064-021-03424-9
39. Li T, Yang J, Yang B, Zhao G, Lin H, Liu Q et al (2020) Ketamine Inhibits Ovarian Cancer Cell Growth by Regulating the lncRNA-PVT1/EZH2/p57 Axis. Front Genet 11:597467. doi: 10.3389/fgene.2020.597467
40. Zhang Z, Sun X, Zhao G, Ma Y, Zeng G (2021) LncRNA embryonic stem cells expressed 1 (Lncenc1) is identified as a novel regulator in neuropathic pain by interacting with EZH2 and downregulating the expression of Bai1 in mouse microglia. Exp Cell Res 399(1):112435. doi: 10.1016/j.yexcr.2020.112435
41. Anwar T, Arellano-Garcia C, Ropa J, Chen YC, Kim HS, Yoon E et al (2018) p38-mediated phosphorylation at T367 induces EZH2 cytoplasmic localization to promote breast cancer metastasis. Nat Commun 9(1):2801. doi: 10.1038/s41467-018-05078-8
42. Yadav R, Weng HR (2017) EZH2 regulates spinal neuroinflammation in rats with neuropathic pain. Neuroscience 349:106–117. doi: 10.1016/j.neuroscience.2017.02.041
43. Yan HL, Sun XW, Wang ZM, Liu PP, Mi TW, Liu C et al (2019) MiR-137 Deficiency Causes Anxiety-Like Behaviors in Mice. Front Mol Neurosci 12:260. doi: 10.3389/fnmol.2019.00260
44. Li J, Gao W, Zhao Z, Li Y, Yang L, Wei W et al (2022) Ginsenoside Rg1 Reduced Microglial Activation and Mitochondrial Dysfunction to Alleviate Depression-Like Behaviour Via the GAS5/EZH2/SOCS3/NRF2 Axis. Mol Neurobiol 59(5):2855–2873. doi: 10.1007/s12035-022-02740-7

Figures

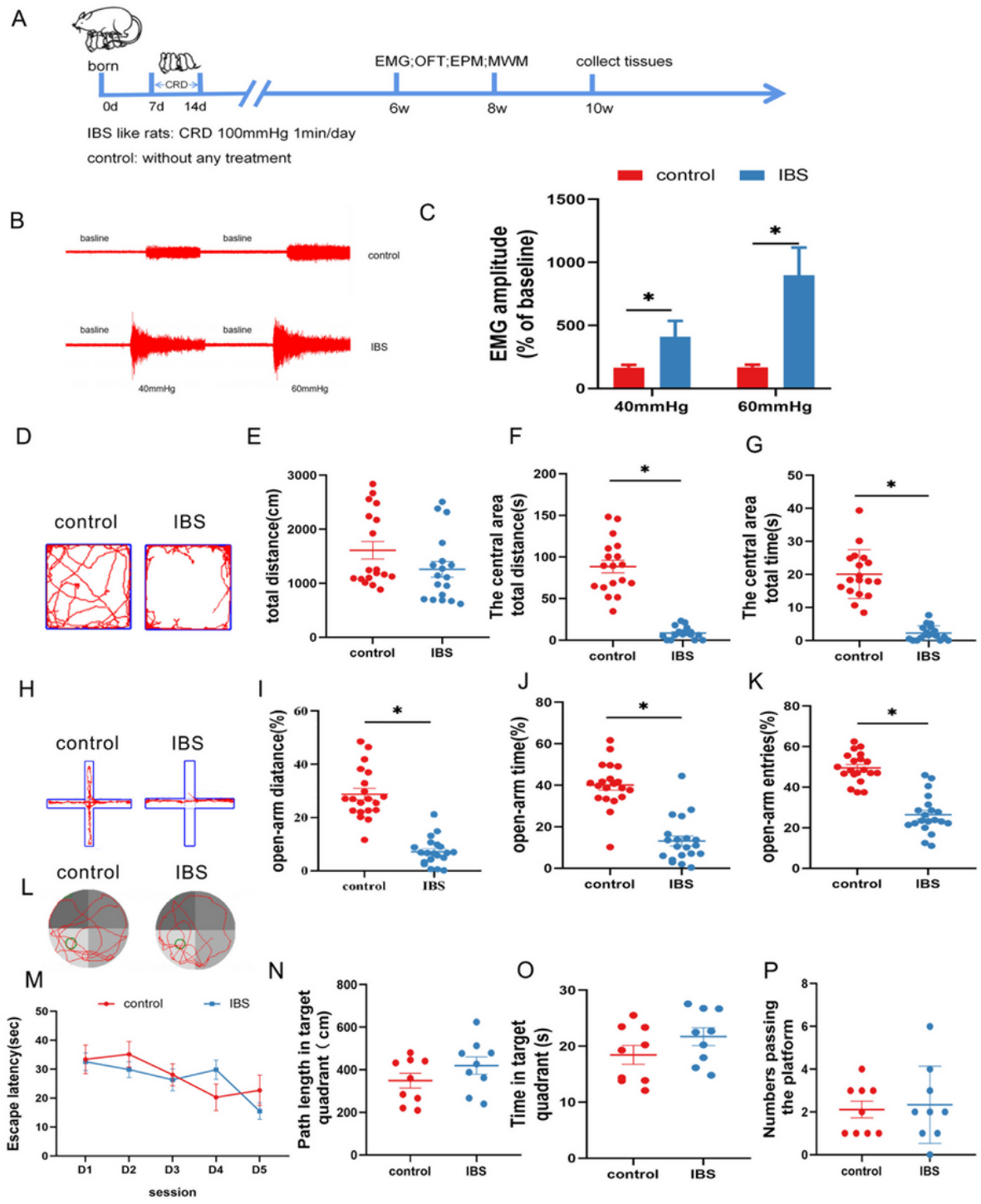

Figure 1

Neonatal CRD induces visceral hypersensitivity and anxiety without cognitive impairment in IBS-like rats. **A** Experimental design. **B** The original typical recordings of EMG under 40 and 60 mmHg CRD in control and IBS-like rats. **C** The statistical chart of the percentage of EMG amplitude over baseline (two-way analysis of variance [ANOVA], n=9, interaction: $F_{(1,32)}$=8.741 **P*<0.05, row factor: $F_{(1,32)}$=31.45 **P*<0.05, column factor: $F_{(1,32)}$=110.7, **P*<0.05). **D** Original typical traces of OFT. Statistical analysis (unpaired t-

test, n = 18) of the total distance (**E**, t= 1.620, df=33.52, *P*=0.1145), the distance in the central area (**F**, t=10.28, df=34, *$P < 0.05$), and the time in the central area (**G**, t=9.792, df=19.97, *$P < 0.05$) in the OFT. **H** Original typical EPM recordings. Statistical analysis (unpaired t-test, n=20) of the distance (**I**, t=8.985, df=29.42, *$P < 0.05$), the time (**J,** t=7.842, df=37.98, *$P < 0.05$), and the number of entries (**K**, t = 8.712, df = 35.47, *$P < .05$) in the open arm of EPM. **L** The original typical recordings of MWM. The statistical chart (unpaired t-test except repeated-measures for escape latency, n=9) of the escape latency (**M**, $P > 0.05$), path length in target quadrant (**N**, t=0.3105, df=13.70, *P*=0.7609), time in target quadrant (**O**, t=1.322, df=15.71, *P*=0.2052), and numbers passing the platform (P, t=1.410, df=15.95, *P*=0.1778) in MWM.

EMG: electromyography; CRD: colorectal distension; OFT: open field test; EPM: elevated plus maze test; IBS: irritable bowel syndrome; MWM: Morris water maze

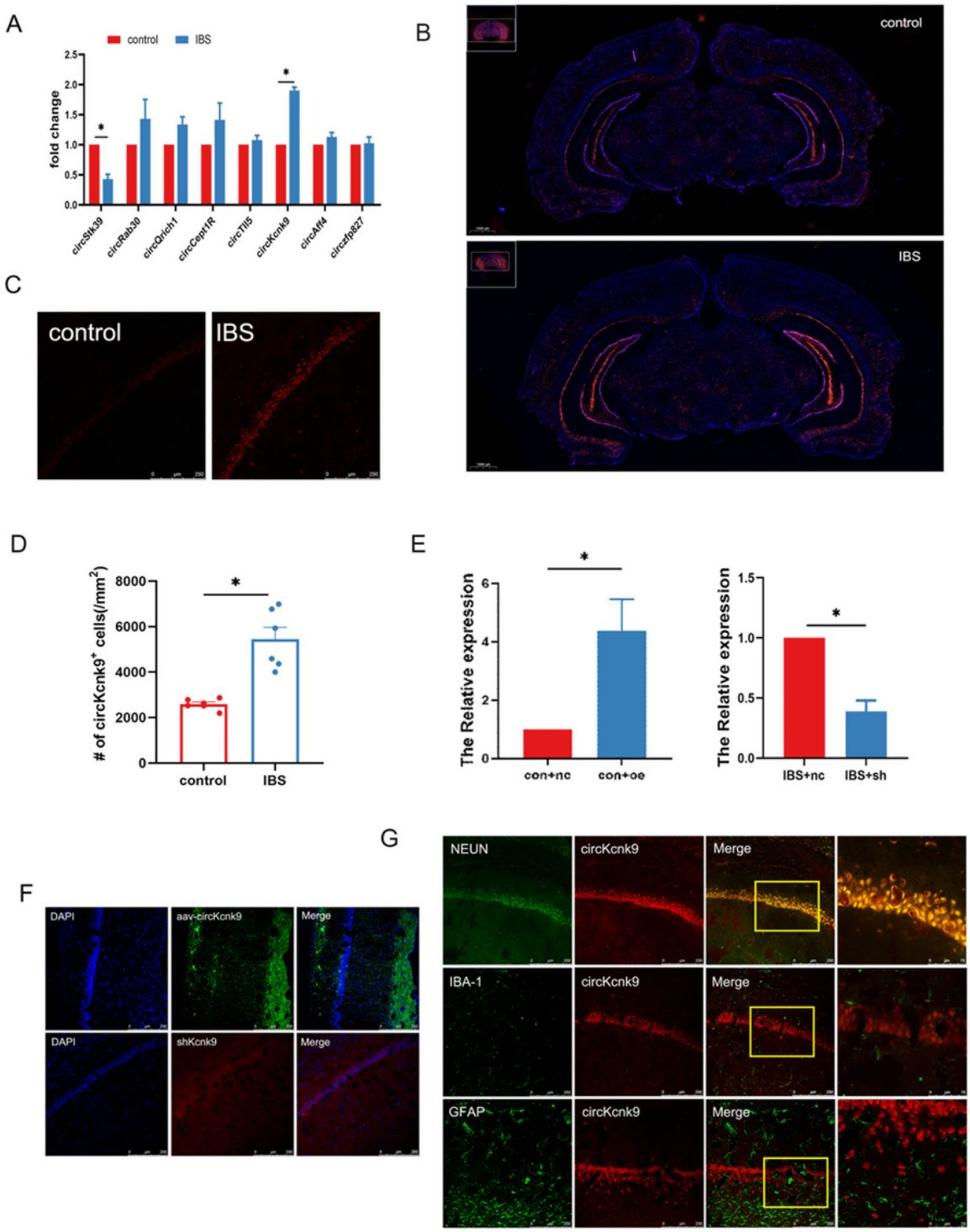

Figure 2

Increased CircKcnk9 is localized in the cytoplasm and nucleus of neurons but not microglia and astrocytes in the hippocampus in IBS rats and the expression of circKcnk9 can be modified after aav-circKcnk9 or shcircKcnk9 treatment. **A** qPCR quantification of the circular RNA associated with chronic visceral pain (Unpaired t-test，n=8, circStk39: t=7.227, df=5.000, *P=0.0008; circKcnk9: t=16.85, df=5.000, *P<0.0001). **B** Distribution map of circKcnk9 content in brain slices (scale bar, 2000μm). Representative

diagram of hippocampal circKcnk9 in IBS-like rats and controls (scale bar, 250μm). Immunofluorescence representative images **C** and quantification (**D**, unpaired t-test, t=5.313, df=5.335 n=6, **P*<0.05) of circKcnk9 numbers in CA1. **E** The expression of CA1 circKcnk9 after treatment with aav-circKcnk9 in controls (Unpaired t-test, n=5, t=3.097, df=4 **P*=0.0363) and shcircKcnk9 in IBS-like rats (t=6.671, df=8, **P*=0.0002). **F** Representative immunofluorescence traces of aav-oe1/shRNA in hippocampal CA1 (scale bar, 250μm). **G** Confocal images of CA1 circKcnk9 expression with NEUN, IBA-1 and GFAP. CircKcnk9 was found colocalized with neuron but not microglia and astrocytes (scale bar, 250μm).

DAPI: nucleus staining dye; PyCL: pyramidal cell layer of the hippocampus

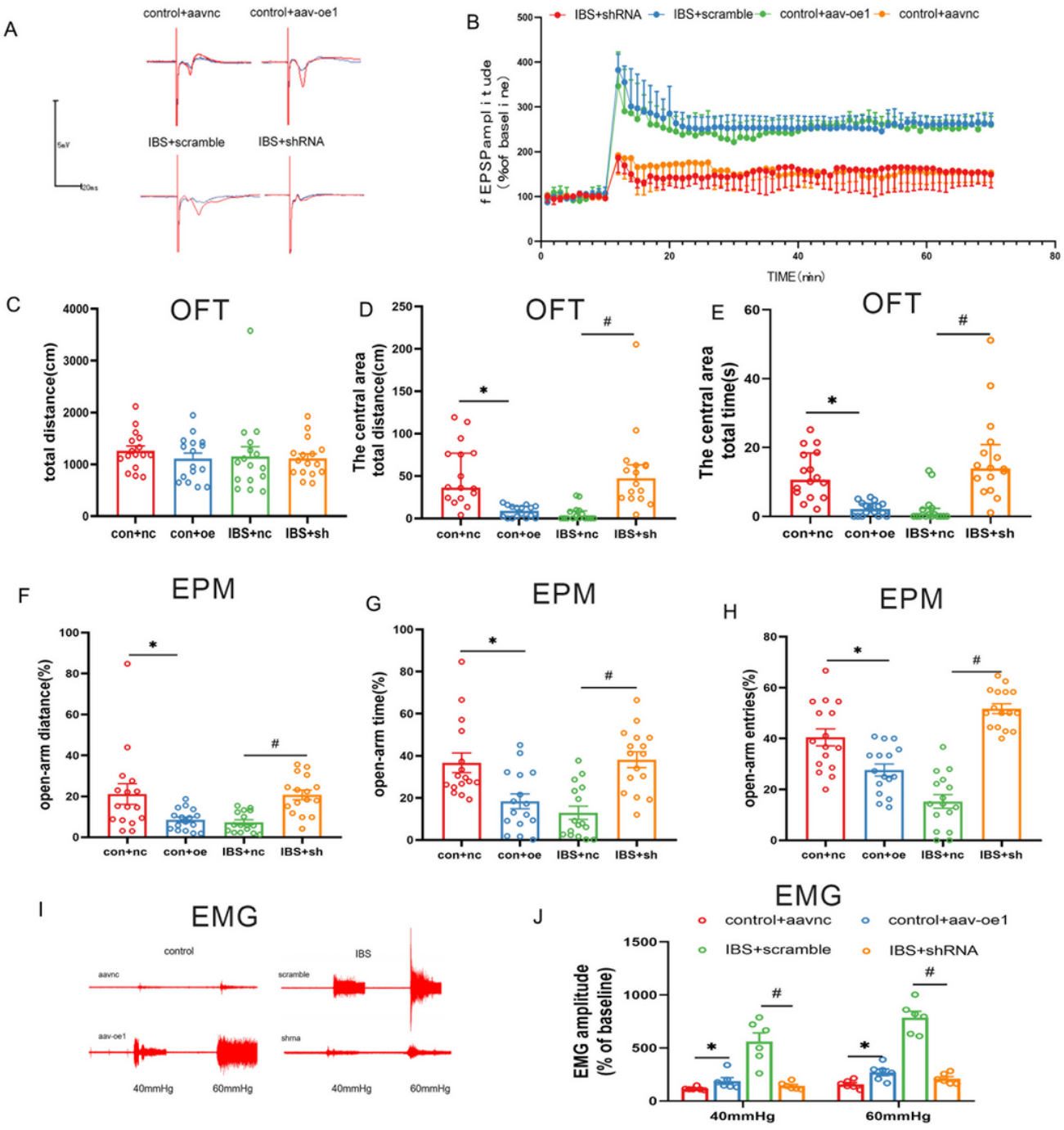

Figure 3

CA1 shcirckcnk9 attenuates LTP, anxiety and visceral hypersensitivity in IBS-like rats while overexpression of CA1 circKcnk9 induces LTP, anxiety and visceral hypersensitivity in controls. Sample waveforms **A** and summary bar charts (**B**, one-way ANOVA repeated-measures, n=3, $F_{(1.300,88.37)}$=303.2, **P*<0.05) of field potential before and 60 min after HFS in the slices of hippocampus. Statistical analysis (n=16) of the total distance (**C**, one-way ANOVA, $F_{(3,60)}$=0.3202, *P*=0.8108), the distance (**D**, rank sum test, Kruskal–Wallis statistic= 38.90, **P*<0.05) and time (**E**, rank sum test, Kruskal–Wallis statistic=38.16, **P*<0.0001) in the central area of the OFT. Statistical analysis (one-way ANOVA, n=16) of the distance (**F**, $F_{(3,60)}$=6.583, **P*=0.0006), the time (**G,** $F_{(3,60)}$=11.22, **P*<0.0001), and the number of entries (H, $F_{(3,60)}$=11.22, **P*<0.0001) in the open arm of EPM. **I** The original typical recordings of EMG under 40 and 60 mmHg CRD. **J** The statistical chart of the percentage of EMG amplitude over baseline (two-way ANOVA, n=6, interaction: $F_{(3,40)}$=2.089, *P*=0.1169; row factor: $F_{(1,40)}$=13.24 **P*=0.0008; column factor: $F_{(3,40)}$=75.40, **P*<0.0001). Shcirckcnk9 was microinjeceted into CA1 to knowdown circKcnk9 in IBS-like rats while aav-circKcnk9 was microinjeceted into CA1 to overexpress circKcnk9 in control rats. 2-3 weeks later, experiments including LTP, OFT, EPM and EMG were performed and differences were compared between the interference and empty-load virus groups.

EPM: elevated plus maze test; OFT: open field test; EMG: electromyography; IBS: irritable bowel syndrome; HFS: high-frequency stimulation; fEPSP: field excitatory postsynaptic; LTP: long-term potentiation;

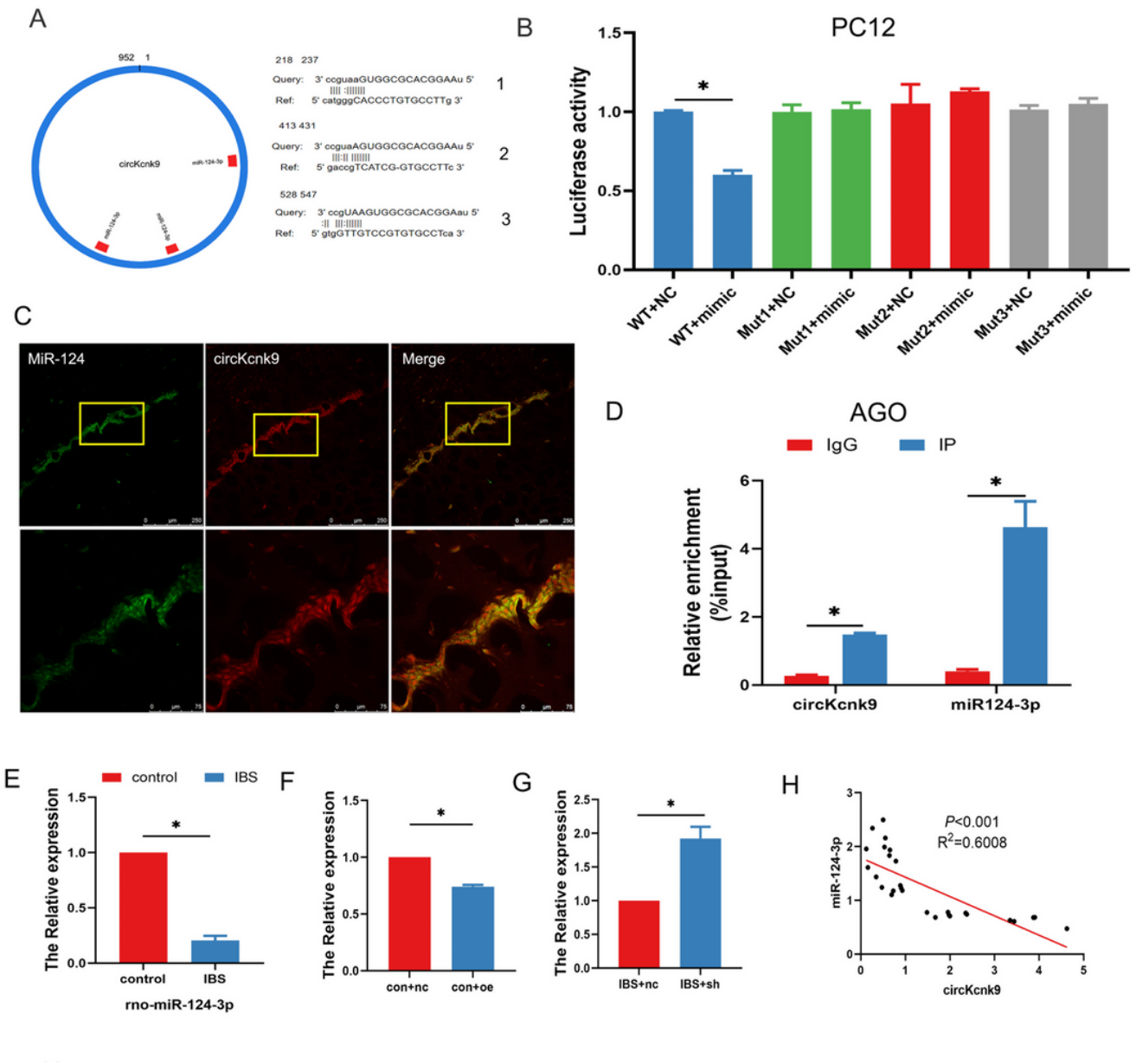

Figure 4

CircKcnk9 acts as miR-124-3p sponge and a negative correlation between them. **A** CircKcnk9 has three binding sites for miR-124-3p. **B** Double-luciferase reporter assay results showed that circKcnk9 could bind to miR-124-3p (unpaired t-test, n=3, t=13.70, df=4, *P*<0.0002). **C** Colocalization of circKcnk9 and miR-124-3p (scale bar, 250μm). **D** AGO protein antibodies can co-precipitate circKcnk9 and miR-124-3p (unpaired t-test, circKcnk9: n=4, t=46.94, df=3, *P*<0.0001, miR-124-3p: t=5.165, df=3, *P*=0.0141). **E** Lower expression of hippocampal miR-124-3p in IBS rats compared with that in controls (unpaired t-test, n=8, t=17.65, df=13, *P*<0.0001). Expression of miR-124-3p after CA1 treatment with aav-circKcnk9 in controls (**F**, unpaired t-test, n=6, t=26.07, df=10, **P*<0.05) and and shcircKcnk9 in IBS-like rats (**G**, t=5.301, df=10, *P*<0.05). **H** Correlation analysis of circKcnk9 and miR-124-3p (*P* <0.05, R^2 =0.6008).

AGO: the vital component of the RNA-induced silencing complex

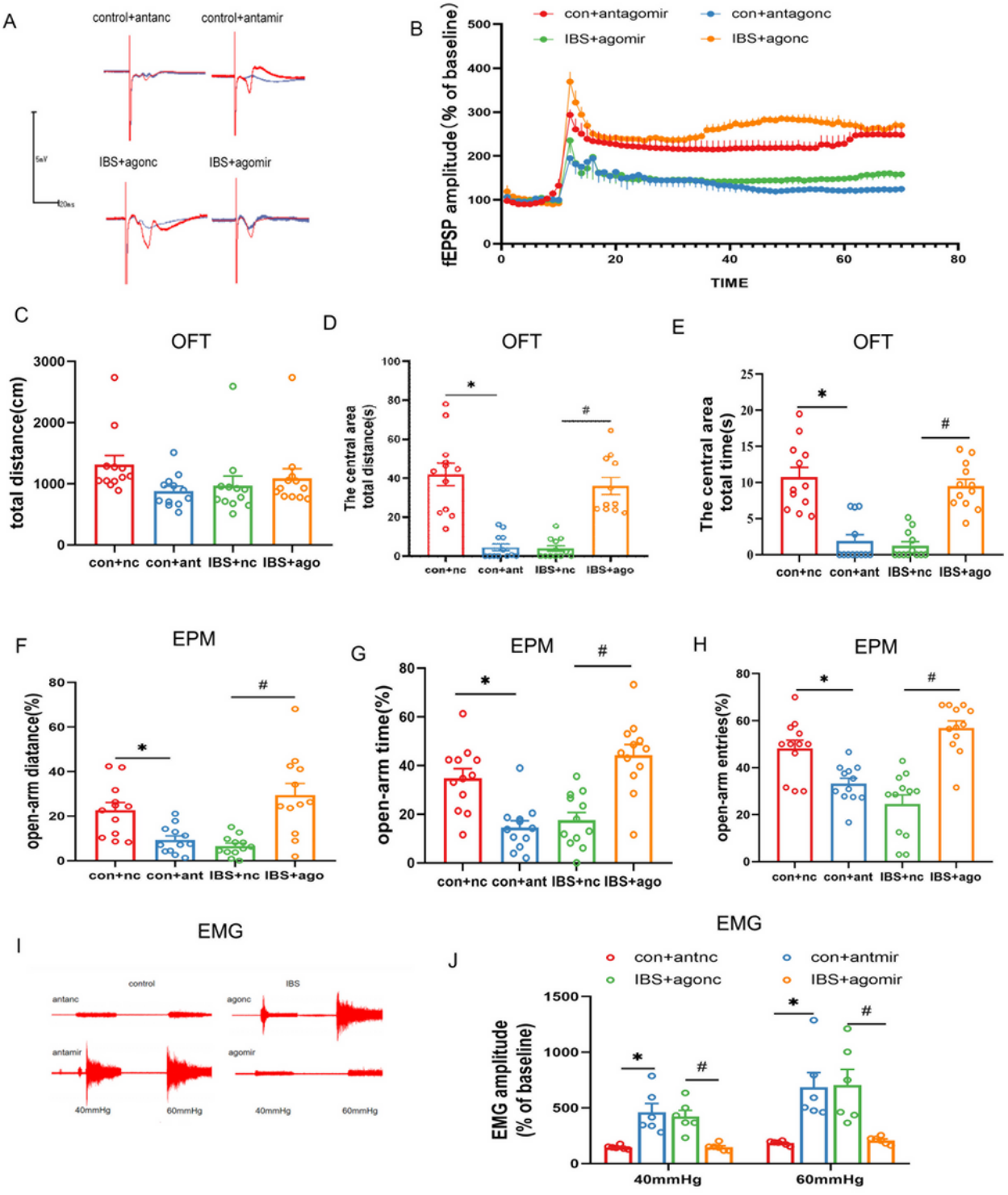

Figure 5

CA1 miR-124-3p upregulation decreased LTP, visceral hypersensitivity and anxiety in IBS-like rats while miR-124-3p blockade induced LTP, visceral hypersensitivity and anxiety in control rats. Sample waveforms **A** and summary bar charts (**B**, one-way ANOVA repeated-measures, n=3, $F_{(1.217,82.77)}$=284.5

*P<0.05) of field potential before and 60 min after HFS in the slices of hippocampus. Statistical analysis (n=12) of the total distance (**C**, one-way ANOVA, n=12, $F_{(3, 44)}$=1.791, P=0.1628), the distance (**D**, rank sum test, Kruskal-Wallis statistic=34.52, P<0.05) and time (**E**, Kruskal-Wallis statistic=33.21, P<0.05) in the central area of the OFT. Statistical analysis (one-way ANOVA, n=12) of the distance (**F**, $F_{(3,44)}$=10.74, P<0.0001), the time (**G,** $F_{(3,44)}$ =15.50, *P<0.0001), and the number of entries (H, $F_{(3,44)}$ = 20.06, *P<0.0001) in the open arm of EPM. (I) The original typical recordings of EMG under 40 and 60 mmHg CRD. (J) The statistical chart of the percentage of EMG amplitude over baseline (two-way ANOVA, n=6, interaction: $F_{(3,40)}$=1.241, P=0.3076; row factor: $F_{(1,40)}$=7.908, *P=0.0076; column factor: $F_{(3,40)}$=18.05, *P<0.0001). AgomiR-124-3p was microinjeceted into CA1 to activate miR-124-3p in IBS-like rats while antagomiR-124-3p was microinjeceted into CA1 to block miR-124-3p in control rats. The microinjection was once a day for 3 days. Then experiments including LTP, OFT, EPM and EMG were performed and differences were compared between the interference and vehicle groups.

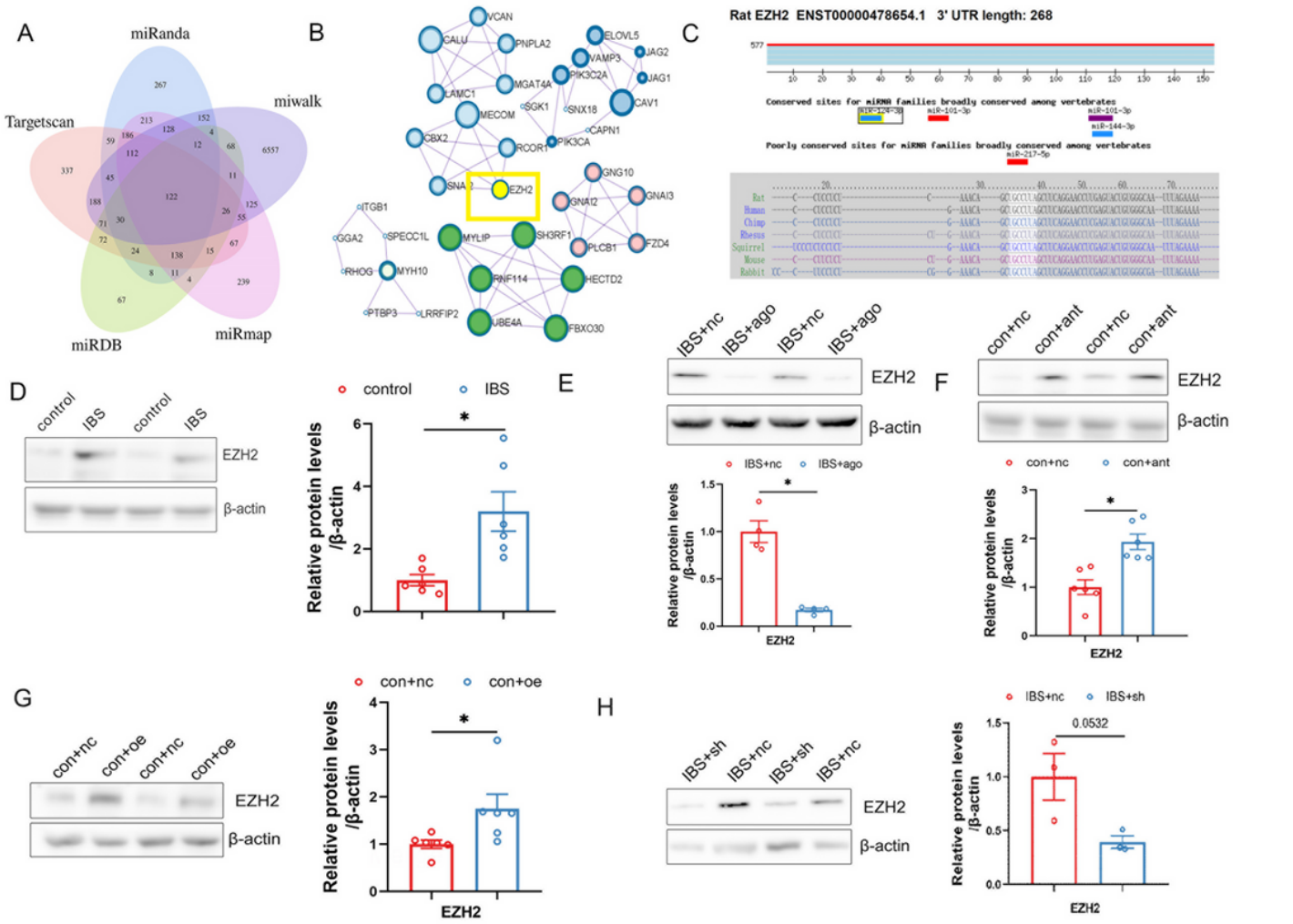

Figure 6

EZH2 is a target gene of circKcnk9/ miR-124-3p and the expression of CA1 EZH2 is regulated by circKcnk9 and miR-124-3p. **A** Interactions between miR-124-3p and its target genes were predicted using TargetScan, microT, miwalk, and Pictar databases. **B** MCODE in Cytoscape candidate target gene PPI network. **C** Sequence conservation of EZH2 binding site for miR124-3p. **D** Representative images (left) and quantification (right) of the EZH2 protein expression in hippocampus of control and IBS-like rats (unpaired t-test, n=6, t=3.350, df=10, **P*=0.0074). Western blot quantification (unpaired t-test) of EZH2 after CA1 treatment of miR-124-3p antagomir in control (**E**, n=6, t=4.265, df=10, **P* =0.0016) and agomir in IBS-like rats (**F**, n=4, t=7.127, df=6, **P*=0.0004). Western blot quantification (unpaired t-test) of EZH2

after CA1 treatment of aav-circKcnk9 in control (**G**, n=6, t=2.339, df=10, *P=0.0414) and shcircKcnk9 in IBS-like rats (**H**, n=3, t=2.716, df=4 , P=0.0532).

MCODE: MCODE network clustering analysis; PPI: protein-protein interaction.

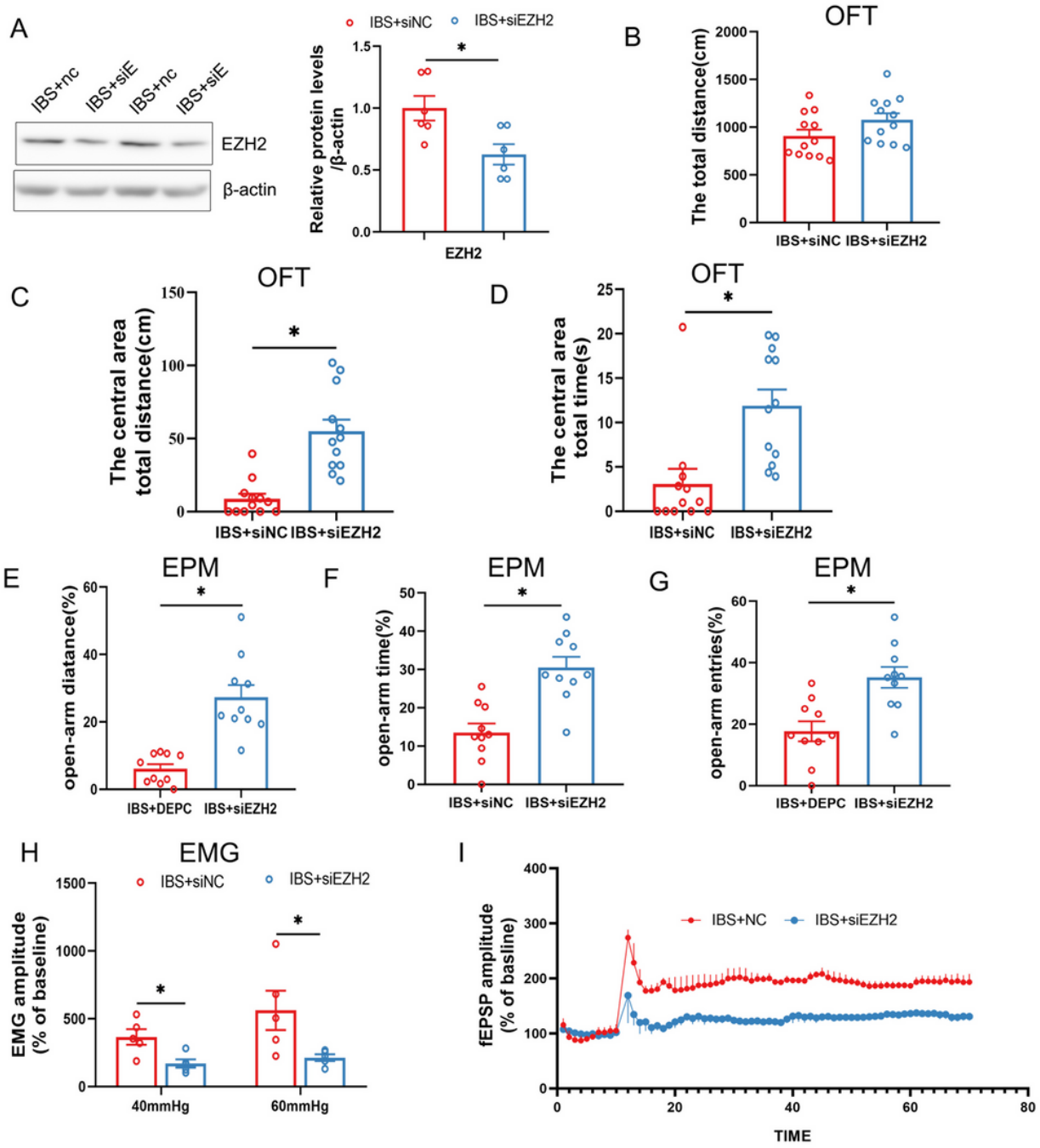

Figure 7

Downregulation of CA1 EZH2 attenuates anxiety, visceral hypersensitivity and LTP in IBS-like rats. **A** EZH2 protein expression decreased after CA1 administration of siEZH2 in IBS-like rats (unpaired t-test, n=6,

t=2.895, df=10, *P=0.0160). Statistical analysis (Unpaired t test, n=12) of the total distance (**B**, t=1.764, df=21.96, P=0.0916), the distance (**C**, t=5.246, df=14.91, *P<0.05) and time (**D**, t=3.555, df=21.87, *P=0.0018) in the central area of the OFT. Statistical analysis (unpaired t test, n = 12) of the distance (**E**, t=5.425, df =11.57, *P=0.0002), the time (**F**, t=4.656, df=17.60, *P=0.0002), and the number of entries **(G**, t=3.726, df=17.95, *P=0.0016) in the open arm of EPM. **H** The statistical chart of the percentage of EMG amplitude over baseline (two-way ANOVA, n=5, interaction: $F_{(1,16)}$=0.8988, P=0.3572; row factor: $F_{(1,16)}$=2.214, P=0.1562; column factor: $F_{(1,16)}$=11.47, *P=0.0038). **I** Summary bar charts (one-way ANOVA repeated-measures, n=3, F= 7.786, DFn=73, Dfd=69, P<0.05) of field potential before and 60 min after HFS in the slices of hippocampus. SiEZH2 was microinjeceted into CA1 to downregulate EZH2 protein expression in IBS-like rats once a day for 3 days. Then experiments including LTP, OFT, EPM and EMG were performed and differences were compared between the interference and vehicle groups.

DEPC: DEPC water; EMG: electromyography; OFT: open field test; EPM: elevated plus maze test; IBS: irritable bowel syndrome; HFS: High frequency stimulation